WORLD CONFERENCE ON TIMBER ENGINEERING 2025
BRISBANE, AUSTRALIA
Advancing Timber for the Future Built Environment

IMPACT BEHAVIOUR OF HYBRID CLT PANELS

Bryan E. Thevarajah[1], Alex M. Remennikov[2], Tuan D. Ngo[3], Hong Guan[4], Benoit P. Gilbert[5]

ABSTRACT: Recent advancements in construction materials have led to an increased interest in Cross-Laminated Timber (CLT) panels as sustainable alternatives to traditional building materials as they are less carbon-intensive and have significant potential for recycling at the end-of-life cycle. The brittle failure mechanisms of CLT can be critical in an extreme loading event and lead to the progressive collapse of the timber building. Combining CLT with high-strength materials in a complementing way could produce a sustainable and resilient hybrid system. This study investigates the performance of CLT panels under dynamic impact loads, focusing on both control panels and hybrid panels strengthened with surface-mounted Carbon Fiber Reinforced Polymer (CFRP) fabric and steel sheets. Commercially available CLT panels were tested using a free-falling drop hammer setup to simulate impact loads of varying intensity. A high-speed data acquisition system recorded impact forces, associated midspan displacements, and strain measurements, while a high-speed camera captured the modes of failure. The experimental setup and methodology enabled a detailed analysis of impact resistance and structural response. Preliminary findings indicate enhanced impact resistance and increased ductility in the CFRP and steel-strengthened CLT panels compared to control panels.

KEYWORDS: cross-laminated timber, ductility, hybrid timber panel, impact

1 – INTRODUCTION

The response of structures subject to impulsive loads remains a field of intense research. During the lifetime of a building, the structure can undergo different kinds of loading conditions and environments. As such, accidental or intentional extreme loading events such as blast explosions or impacts from debris can initiate catastrophic failures which can cause loss of life and damages. Whilst traditional construction materials, such as steel and concrete, have been the focus of most studies, further research on the performance of alternative materials for blast- and impact-resistant applications has been driven by their growing use in sustainable construction. As the use of more sustainable building materials is increasing, the likelihood to build taller buildings is also increased as evidenced by the allowance of timber buildings up to 25 metres for all classes of buildings in 2019 [1]. As the use of cross-laminated timber (CLT) systems becomes more popular in taller buildings, the chances of exposure to deliberate blast threats and accidental gas explosions or impacts are increased. Since it is a new building approach, mass solid timber systems are susceptible to a lack of robustness and structural resilience as evidenced by the collapse of timber structures in Germany, Denmark, and Finland. Some major reasons for such progressive collapses are found to be the brittle behaviour and comparatively low

[1] Bryan Eric Thevarajah, School of Civil, Mining, Environmental, and Architectural Engineering, The University of Wollongong, Wollongong, Australia, tbryan@uow.edu.au

[2] Alex M. Remennikov, School of Civil, Mining, Environmental, and Architectural Engineering, The University of Wollongong, Wollongong, Australia, alexrem@uow.edu.au

[3] Tuan D. Ngo, Department of Infrastructure Engineering, The University of Melbourne, Parkville, Australia, dtngo@unimelb.edu.au

[4] Hong Guan, School of Engineering and Built Environment, Griffith University, Gold Coast, Australia, h.guan@griffith.edu.au

[5] Benoit Gilbert, School of Engineering and Built Environment, Griffith University, Gold Coast, Australia, b.gilbert@griffith.edu.au

https://doi.org/10.52202/080513-0064

stiffness of the timber structural members, and the low ductile behaviour of the connections [2, 3]. This underlying limitation of the timber products is exaggerated and can be considered to have extreme importance in the event of high-strain rates which are associated with impulsive loading [4].

Not only increasing the thickness of the CLT may not be an economically preferred solution but also less effective [5]. Enhancing CLT with high-strength materials like steel and fibre-reinforced polymer (FRP) can produce hybrid systems with improved ductility and energy absorption [6-11]. Full-scale live-blast testing of a two-storied CLT building was conducted by Weaver, Newberry et al. [12] investigating the response of CLT structures, components, and connections to mimic real-world scenarios. The performance and behaviour of CLT panels have been extensively studied under simulated blast loading in shock tubes focusing on the flexural behaviour, connections, and methods to model the response and effects of retrofitting with fibre-reinforced polymer fabrics [6, 8, 10, 13-17]. Flores, Gentry et al. [4] investigated the behaviour of CLT panels under impulsive loads simulated by the ultra-high-velocity actuator and low span-to-depth ratio between 6.4 and 6.55. Despite extensive studies on the hybrid timber systems under static, cyclic and blast load conditions, there is still a lack of knowledge in the area of the impact performance of CLT and hybrid CLT systems. This study aims to investigate the behaviour of CLT and hybrid CLT panels under impact loading conditions.

2 – EXPERIMENTAL PROGRAMME

2.1 Experimental setup

Dynamic impact tests were performed using the high capacity drop hammer facility at the University of Wollongong. The facility includes a 600 kg free-falling weight with a 250 mm diameter cylindrical tup and a dynamic load cell rated for forces up to 1200 kN. The hammer can be raised to heights of up to 6 m using an electric motor and released via a quick release mechanism, generating impact energies between 1 kJ and 35 kJ. The CLT panel samples were simply supported on two 300PFC (parallel flange channel) sections with clear spans of 1600 mm. The steel supports were bolted to the strong floor to ensure stability during testing. To prevent panel rebound under impact loads, the panels were secured to the supports using ratchets and straps and positioned carefully to avoid adding any restraints against the applied impact forces. The experimental setup and the schematic of the experimental setup are presented in Fig. 1.

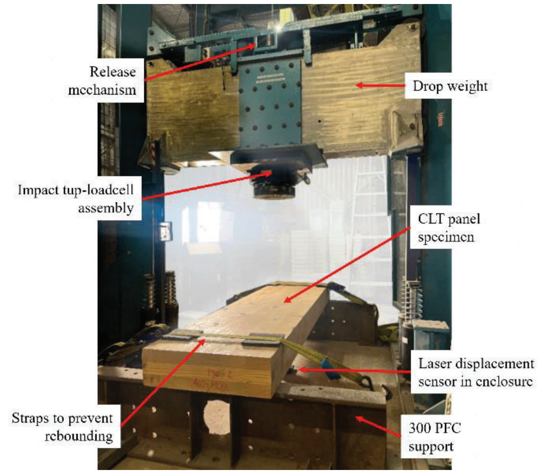

Figure 1. Dynamic impact test setup

A high-speed data acquisition system (NI cDAQ-9174 with NI 9235, 9205, 9207 bridges) was used to capture all test data, including impact forces from the dynamic load cell and midspan displacements measured by a laser displacement sensor positioned beneath the CLT panels. Data were recorded at a sampling rate of 10,000 samples per second. The data logging was started with an automated laser trigger system which is triggered when the drop hammer reaches about 400 mm above the sample ensuring the capture of the data from the initial impact. The duration of the data collection was specified to be 5 seconds from the beginning of the data collection. Additionally, an NAC MEMRECAM HX-7 high-speed camera recorded the impact events at 5000 frames per second, providing detailed footage for post-test analysis of failure mechanisms and damage progression. The high-speed camera images were also utilised to measure displacement when the laser displacement measurement was out of range.

2.2 Specimens

A total of 11 CLT panel samples were tested under dynamic impact loading and grouped into three categories based on panel thickness. The nomenclature of specimen labelling reflects the dynamic test sample number, number of layers, panel thickness, and hybridization method, e.g., D03-CLT3-76-S0.8 refers to a 3-layer panel with a thickness of 76 mm hybridized with 0.8 mm steel sheet. Similarly, BL indicates baseline panels, CFRP indicates panels strengthened with CFRP fabric, and S3 indicates panels strengthened with a 3 mm thick steel sheet. A series of dynamic impact tests were conducted to allow observations under exceeding extreme impact energies. Drop heights were selected to

https://doi.org/10.52202/080513-0064

allow varied levels of damage ranging from inelastic to complete failure.

Three groups of CLT panels were tested under varying impact energies. Each group except CLT5-220 included a baseline panel and hybrid configurations strengthened with CFRP, 0.8 mm steel, and 3 mm steel. The CLT5-220 group included only a baseline panel, and a panel strengthened with CFRP fabric. The impact energies ranged from 2.7 kJ for baseline panels to over 11 kJ for hybrid panels, with higher velocities assigned to stronger configurations. The details of the experimental programmes are summarised in Table 1. In this study, the drop hammer weight was kept constant at 600 kg. Various drop heights were selected to achieve different impact velocities, resulting in a range of impact energies. The required heights to achieve the target velocities are obtained from the energy equation as in (1).

$$h = \frac{V^2}{2g} \tag{1}$$

where: h is drop height; V is final impact velocity; and g is the gravitational acceleration.

3 – RESULTS AND DISCUSSION

The moisture content of the tested CLT panels was measured using the oven-dry method from specimens extracted from the samples post-testing. An average moisture content of 13.5% with a corresponding coefficient of variation (COV) of 4.08 was recorded.

3.1 Failure modes

The baseline panel from the CLT3-76 group (D01-CLT3-76-BL) failed by brittle tension failure, which initiated at a knot and spanned across through finger joints in a staggered path. The failure propagated to the top layers resulting in a complete collapse. In D02-CLT3-76-CFRP the failure mode was similarly tension dominated with gradual progression. Tension cracking initiated in the bottom layer mainly following a staggered path of finger joints which caused CFRP rupture and delamination. The cracks extended to the top layers through glue lines eventually leading to complete collapse. D03-CLT3-76-S0.8 exhibited a combination of tension and rolling shear failures. While tension cracks were mainly focused on finger joints, rolling shear developed in the middle transverse layer. Although slight delamination was observed near failure, the steel sheet yielded locally and prevented the complete collapse of the panel. The panel specimen D04-CLT3-76-S3, recorded a rolling shear and glue line failure between layers. Cracks in the compression layer were recorded however, the panel retained integrity without collapse. Steel sheet separation was observed near the supports. The failure modes of the panels are presented in Fig. 2.

The baseline CLT3-130 panels D05-CLT3-130-BL and D05a-CLT3-130-BL, failed predominantly in tension where the panel with finger joints exhibited a staggered failure path while the panel without finger joints recorded an almost straight failure path connecting knots. Both panels experienced full collapse under the applied impact load. In panel D06-CLT3-130-CFRP, the failure initiated with rolling shear failure in the transverse middle layer followed by tension failure of the bottom layer and CFRP rupture. Although the CFRP fabric delayed the failure, the delamination of CFRP eventually led to the complete collapse of the panel. In both D07-CLT3-130-S0.8 and D08-CLT3-130-S3 panels, failure initiated as a combination of glue line and rolling shear failures.

Table 1. Summary of the experimental programme

Sample No.	Dimension	Layer thicknesses (mm)	Impact velocity (m/s)	Impact energy (J)
D01-CLT3-76-BL	500x2000	25/26/25	3.0	2,700
D02-CLT3-76-CFRP	500x2000	25/26/25	5.0	7,500
D03-CLT3-76-S0.8	500x2000	25/26/25	5.0	7,500
D04-CLT3-76-S3	500x2000	25/26/25	5.0	7,500
D05a-CLT3-130-BL	460x1900	42.5/45/42.5	4.0	4,800
D05-CLT3-130-BL	460x1900	42.5/45/42.5	4.0	4,800
D06-CLT3-130-CFRP	480x1900	42.5/45/42.5	5.5	9,075
D07-CLT3-130-S0.8	480x1900	42.5/45/42.5	5.7	9,747
D08-CLT3-130-S3	460x1900	42.5/45/42.5	6.1	11,163
D09-CLT5-220-BL	440x1900	42.5/45/45/45/42.5	4.5	6,075
D10-CLT5-220-CFRP	450x1900	42.5/45/45/45/42.5	6.0	10,800

https://doi.org/10.52202/080513-0064

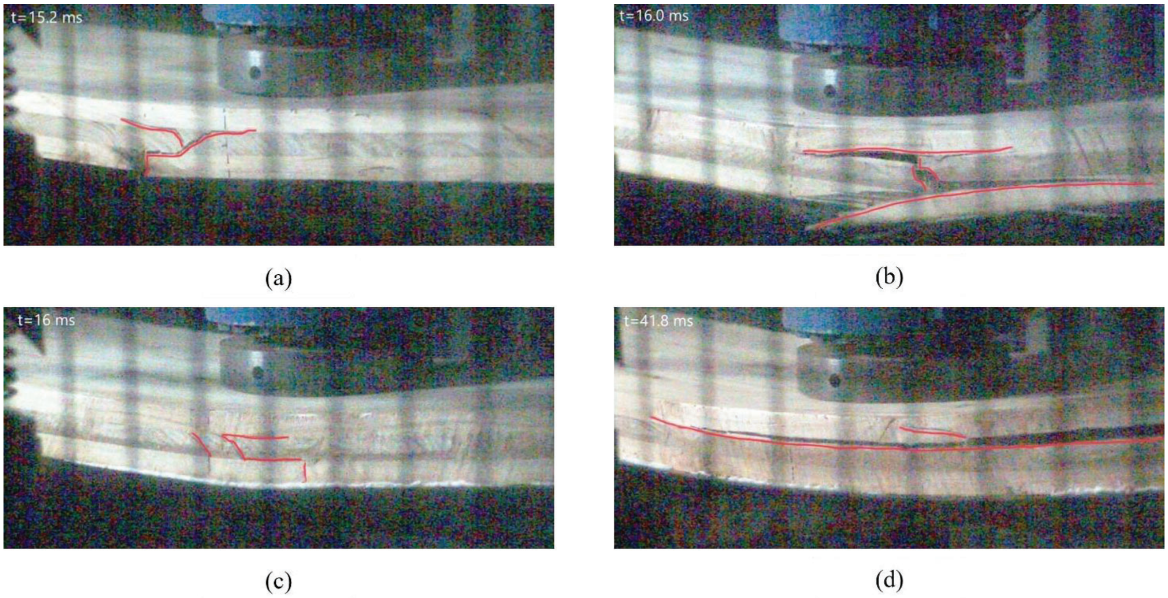

Figure 2. Failure modes (a) D01 - Tension failure; (b) D02 – Tension and glue line failure; (c) D03 – Rolling shear and tension failure; (d) D04 – Glue line failure

The final collapse of D08-CLT3-130-S3 was initiated by compression crushing and tension failure following the detachment of the 3 mm steel sheet. In D07-CLT3-130-S0.8, although tension failure occurred, the yielding of the steel allowed the panel to retain limited residual capacity despite extensive damage. The failure modes of the CLT3-130 panels are shown in Fig. 3.

The baseline panel of CLT5-220 (D09-CLT5-220-BL) failed primarily in tension, initiating in the outermost longitudinal layer and spanning across in a staggered path following finger joints and knots. The cracks propagated to the subsequent transverse and longitudinal layers along glue lines. Rolling shear was observed in the top transverse layer as the failure propagated. Despite the damage the panel demonstrated some residual capacity to

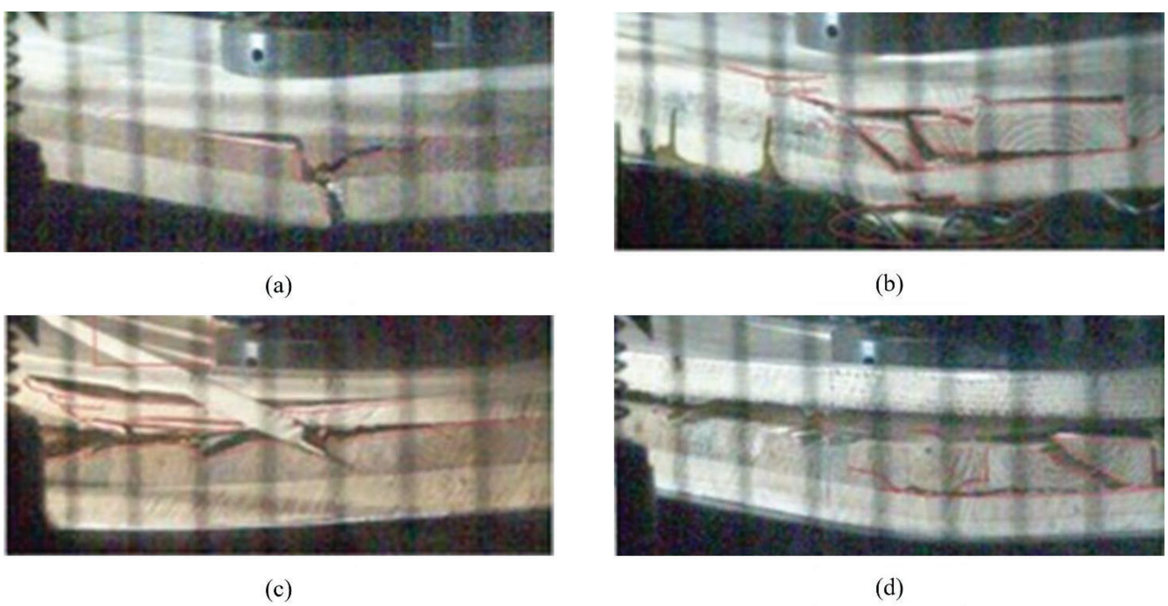

Figure 3. Failure modes (a) D05a – Tension failure; (b) D06 – Rolling shear and tension failures; (c) D07 – Glue line and compression crushing failures; (d) D08 – Rolling shear failure

support the weight of the drop hammer as the hammer came to a rest dissipating all the potential energy. In contrast, panel D10-CLT5-220-CFRP exhibited an initial failure by rolling shear in both transverse layers followed by tension failure in the bottom longitudinal layer. However, the tension failure did not propagate to the adjacent layers. The CFRP fabric was observed to be ruptured around the tension failure of timber i.e. finger joints. The sample exhibited sufficient capacity as the hammer was observed to rebound without the collapse of the sample. The failure modes of the CLT5-220 panels are illustrated in Fig. 4.

3.2 Impact load time histories

When subjected to an impact load from a falling mass, the sample resists the dynamic impact forces through a combination of inertial and flexural resistance mechanisms [18-20]. The dynamic equilibrium of the panels can be expressed in (2). Upon impact, the panel accelerates in the direction of the applied force, generating inertial loads in the opposite direction. This acceleration leads to a brief separation between the drop hammer and the panel. The hammer then catches up, contacting the sample again. These rebounding cycles occurred 2-3 times before the hammer and panel moved in unison, allowing the remaining impact force to be fully applied.

$$\int_0^L \bar{m}\ddot{u}(x,t)\,dx + R(t) = F(t) \tag{2}$$

where L is the length of the panel, $\bar{m}$ is the mass per unit length, $\ddot{u}$ is the acceleration at any point of the panel, R is the support reactions, and F is the impact force.

The dynamic load-time history responses exhibited two distinct behaviours across the samples. All the panels initially recorded 2-3 rapid peaks and drops corresponding to the inertial resistance and momentary separation due to samples accelerating away from the drop hammer. This was confirmed by comparing the dynamic load-time histories with high-speed camera recordings. The maximum load recorded is referred to as the maximum impact force (F_m). After the initial inertial peaks, the drop hammer and the panel moved together without separation and the impact load-time history recorded an almost constant load over a longer duration. This constant load is referred to as plateau impact force (F_p) which is determined according to the (3) and the corresponding duration is referred to plateau duration (t_p) [21, 22]. During this period, the sustained impact load is primarily resisted by the bending capacity of the beam, with little contribution from inertial resistance [19, 20, 23]. This was also confirmed by evaluating the acceleration at the midspan which remained close to zero [24, 25]. While the plateau impact force has been used as an indicator of dynamic impact resistance in concrete and steel beams, in this series of experiments, fracture of CLT was observed in the samples during the peaks caused by inertia before plateau stage. Therefore, the plateau forces can only be used for comparison purposes in this study as opposed to determine the impact bending resistance of the panels as fractures in CLT can lead to reduction of resistance [19, 21, 25-27].

The plateau stage was followed by a decaying stage over a decaying duration (t_d), where the impact force was decreasing gradually to zero as the drop hammer rebounds and separates from the panel. The duration between the initial contact and rebound (when impact load reaches zero) of the drop hammer is defined as the impact duration (t_i). Fig. 5 shows the definitions of the characteristic values of a typical impact load-time history.

$$F_p = \int_{t_1}^{t_2} \frac{F(t)dt}{t_2 - t_1} \tag{3}$$

where t_1, t_2 corresponds to the start and end time of the plateau stage respectively.

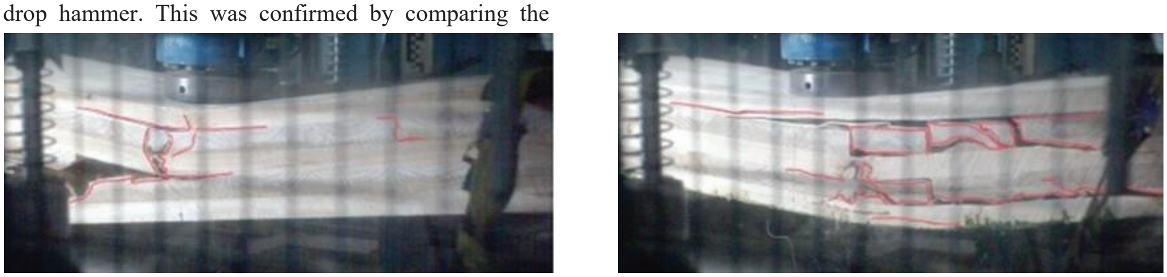

(a) (b)

Figure 4. Failure modes (a) D09 – Tension and rolling shear failures; (b) D10 – Rolling shear and tension failure

https://doi.org/10.52202/080513-0064

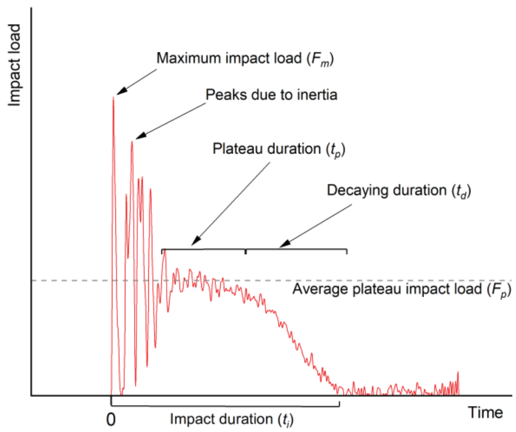

Figure 5. Definition of characteristic values in an impact-time history

In contrast, the panels that collapsed under dynamic loads exhibited different responses following the initial inertial stage. In these panels, a definite plateau stage was not clearly identified as the samples started to collapse after the inertial peak loads. Followed by the inertial peaks no distinct plateau stage was observed, preventing a clear comparison of the performance under dynamic impact loads from the load-time histories. Table 2 presents the characteristic values from the impact load-time histories of the tested samples.

As described in the previous section, all hybrid panels from the CLT3-76 thickness were subjected to equal impact energies, whereas the baseline panel was subjected to a lower impact energy. While the baseline sample and the CFRP strengthened panel (D01-CLT3-76-BL and D02-CLT3-76-CFRP) collapsed without exhibiting a plateau stage under the applied impact loads, both panels strengthened with 0.8 mm and 3 mm steel (D03-CLT3-76-S0.8 and D04-CLT3-76-S3) recorded notable plateau stages with varying characteristics. These results suggest that hybridizing with steel provides a better enhancement of impact resistance to CLT than CFRP to sustain the load and prevent a catastrophic sudden failure. For an equal impact energy of 7500 J, D04-CLT3-76-S3 recorded longer plateau (t_p) and decaying (t_d) durations resulting in a longer impact load duration (t_i) than D03-CLT3-76-S0.8. Sample D04-CLT3-76-S3 recorded about 40, 25, and 26 % increases respectively in t_p, t_d, and t_i compared to sample D03-CLT3-76-S0.8. As the impact load duration increased, the plateau load recorded a reduction of 17 % when the thickness of the steel was increased. This suggests better energy dissipation at the expense of flexural resistance possibly due to glue line failure of timber and separation between steel and timber.

Due to a malfunction in triggering data logging, impact load and displacement data from DAQ were not recorded during the testing of D05a-CLT3-130-BL. In CLT3-130 panels, although the samples D06-CLT3-130-CFRP and D08-CLT3-130-S3 did not exhibit a plateau stage, the load-time history recorded a noticeable decaying stage towards failure compared to the baseline sample D05-CLT3-130-BL which showed neither any clear plateau nor decaying stage for a lower level of impact energy. This indicates an improvement in impact resistance when strengthened with CFRP and a 3 mm steel sheet. Sample D07-CLT3-130-S0.8 recorded a higher load of 88.5 kN for a brief duration of 2.5 ms and as the failure propagated the plateau load settled at a lower load of 44.4 kN which lasted for about 45.5 ms duration indicating enhanced resistance and energy dissipation.

Both CLT5-220 samples did not exhibit a distinct plateau stage compared to sample D03-CLT3-76-S0.8. Sample D09-CLT5-220-BL exhibited a noticeable decay stage after the inertial peaks indicating rapid degradation of resistance. Since the drop hammer came to rest without rebounding supported by the residual capacity of the panel, the load cell continued to record the weight of the drop hammer, preventing the estimation of decay or impact duration. Sample D10-CLT5-220-CFRP oscillated at a higher magnitude of load (35–143 kN) after inertial peaks than the baseline counterpart D09-CLT5-220-BL (19–73 kN) indicating some enhancements in impact resistance.

3.3 Displacement time histories

The midspan displacement-time responses of the CLT samples under the dynamic impact loading are categorised by the thickness of CLT and presented in Fig. 6. In all the panels, a lag of around 0.3 – 0.9 ms was observed between first contact and initiation of displacement. This indicates the initial inertial resistance to the impact. Generally, a parabolic curved response was recorded up to the peak displacement across the samples. The panels that collapsed under the applied impact loads, exhibited only a positive decreasing displacement rate up to the peak/failure of the panels during which period the drop hammer and the sample are in contact and moving together. In panels that rebounded due to insufficient impact energy to cause a complete collapse, a two-part behaviour was observed. Like the collapsed panels, the first part of the response represents a unison movement between the drop hammer and the sample up to the peak displacement. As the applied impact energies were not sufficient to initiate a complete failure, the samples rebounded and moved upwards.

In CLT3-76 panels, the baseline panel D01-CLT3-76-BL, collapsed under an impact energy of 2697 J. The reinforced panels when subjected to an increased impact energy of 7495 J, while the panels strengthened with steel rebounded, CFRP strengthened D02-CLT3-76-CFRP also collapsed. Although the panel reinforced with 0.8 mm steel - D03-CLT3-76-S0.8, reached a maximum deflection of 94.1 mm, compared to the maximum deflection of 82.3 mm of 3 mm steel panel – D04-CLT3-76-S3, the 3 mm steel reinforced panel returned almost completely to its original position despite of glue line failure in CLT, while the 0.8 mm steel reinforced panel exhibited a residual displacement of 45.6 mm suggesting more ductile behaviour of 0.8 mm steel reinforced panel.

All samples in the CLT3-130 group completely collapsed under the applied impact loads except D07-CLT3-130-S0.8, which rebounded although extensive failure was observed in CLT. The panel rebounded back to a permanent displacement of 109.9 mm after reaching a peak deflection of 139.9 mm. The displacement history presented for sample D05a-CLT3-130-BL was obtained by image processing the high-speed camera recordings as the data was not recorded on the high-speed DAQ system. The baseline panel D09-CLT5-220-BL collapsed under the impact energy of 6075 J, while CFRP reinforced panel D10-CLT5-220-CFRP exhibited a maximum displacement of 74.5 mm and a permanent deflection of 9.4 mm for an increased impact energy of 10800 J.

3.4 Energy absorption

The energy absorbed by each sample subjected to dynamic impact loading was estimated from the area beneath the impact load-displacement curves [27, 28]. As most panel samples experienced complete collapse under dynamic forces, the calculated energy absorption reflects the capacity up to the total collapse, including post-peak energy absorption. However, this may not be the case for the panel samples that did not exhibit a complete collapse such as D03-CLT3-76-S0.8, D03-CLT3-76-S3, D07-CLT3-130-S0.8, and D10-CLT5-220-CFRP as the panels would still be able to absorb energy after initial failure [29]. Fig. 7 presents the energy absorption capacities.

As expected, unreinforced baseline panels exhibited the lowest energy absorption across all the thicknesses considered with corresponding capacities of 2321, 3690, and 6042 J for CLT3-76, CLT5-130, and CLT5-220 respectively. Reinforced panels showed significantly enhanced energy absorption compared to their baseline counterparts. For CFRP-reinforced panels, energy absorption increased by 69 % for CLT3-76, 87 % for CLT3-130, and 58 % for CLT5-220.

Table 2. Characteristic values of impact load-time histories and failure modes

Sample	Impact energy (J)	F_m (kN)	t_i (ms)	F_p (kN)	t_p (ms)	t_d (ms)	*Failure mode*
D01-CLT3-76-BL	2,700	94.3	-	-	-	-	Tension (finger joint) – glue line
D02-CLT3-76-CFRP	7,500	155.7	-	-	-	-	Tension (finger joint) – glue line - delamination
D03-CLT3-76-S0.8	7,500	205.9	73.2	59.4	24.2	33.4	Rolling shear - tension (finger joint)
D04-CLT3-76-S3	7,500	189.2	91.9	49.3	33.8	41.6	Rolling shear – glue line - delamination - compression
*D05-CLT3-130-BL	4,800	-	-	-	-	-	Tension (finger joints) - rolling shear
D05-CLT3-130-BL	4,800	170.3	-	-	-	-	Tension – glue line
D06-CLT3-130-CFRP	9,075	349.4	33.4	-	-	22.6	Rolling shear - tension (finger joint) - delamination
D07-CLT3-130-S0.8	9,747	366.7	100.8	44.4	45.5	37.3	Glue line - rolling shear - tension
D08-CLT3-130-S3	11,163	329.8	37.5	-	-	30.8	Rolling shear – glue line - compression
D09-CLT5-220-BL	6,075	356.0	-	-	-	-	Tension - rolling shear - tension
D10-CLT5-220-CFRP	10,800	465.0	75.6	-	-	44.0	Rolling shear - tension (finger joint)

*Data not acquired due to a technical issue.

https://doi.org/10.52202/080513-0064

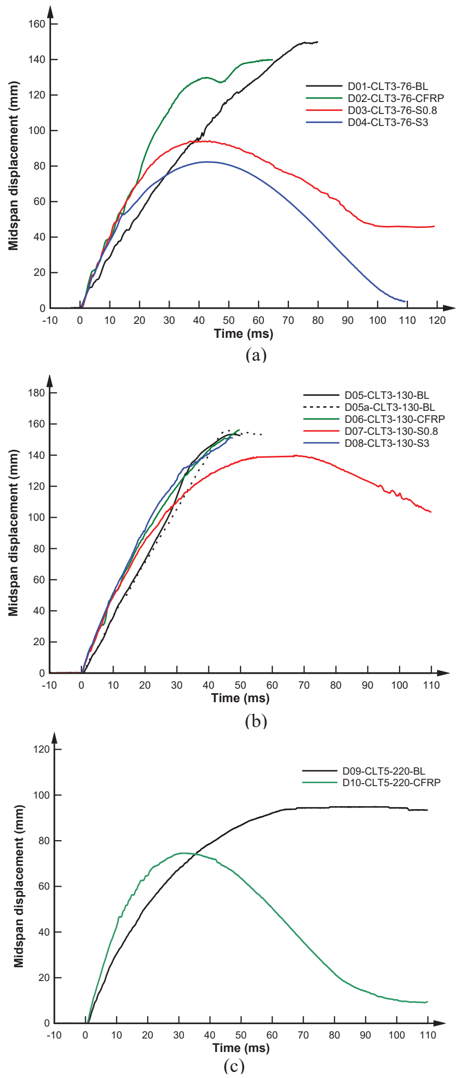

Figure 6. Displacement time histories (a) CLT3-76; (b) CLT3-130; (c) CLT5-220

Samples reinforced with 0.8 mm steel exhibited the highest energy absorption across the thicknesses surpassing CFRP and 3.0 mm steel reinforced samples. CLT3-76 panels reinforced with 0.8 mm steel showed a 142 % increase compared to the baseline, and CLT3-130 samples saw a 154 % for CLT3-130 sample. 3 mm steel reinforcement offered a higher energy absorption capacity than baseline and CFRP samples, although slightly lower than 0.8 mm steel. This difference is possibly due to premature rolling shear and compression layer failures in the CLT. For CLT3-76 reinforced with 3 mm steel, energy absorption increased by 98 %, while CLT3-130 showed a 150 % increase.

Fig. 8 shows the variation of energy absorption capacity against the thickness of CLT across both baseline and reinforced panels. Generally, thicker panels exhibited higher energy absorption capacity, suggesting that the panel thickness positively correlates with energy absorption capacity. Although the sample size is limited, the energy absorption capacity of the baseline panels was observed to increase linearly with thickness. While increasing panel thickness can enhance energy absorption, it may not be the most economically viable approach, especially given its limited impact on improving load resistance capacity as demonstrated by Navaratnam, Christopher et al. [5]. In CFRP-strengthened panels, a steeper increase was observed from CLT3-76 to CLT3-130 than in baseline samples. However, a less steep increase similar to what was observed in baseline samples was observed between CLT3-130 and CLT5-220 panels. There could be two possible explanations. First, as stated earlier the reported

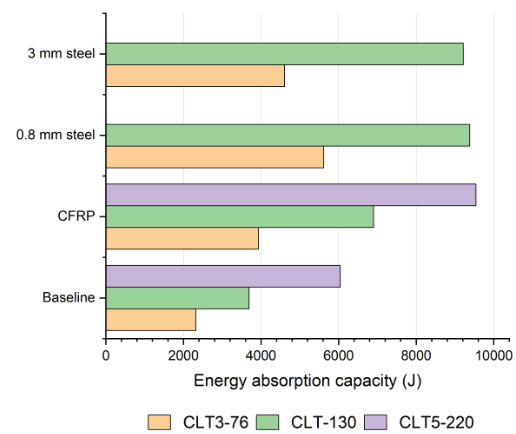

Figure 7. Energy absorption

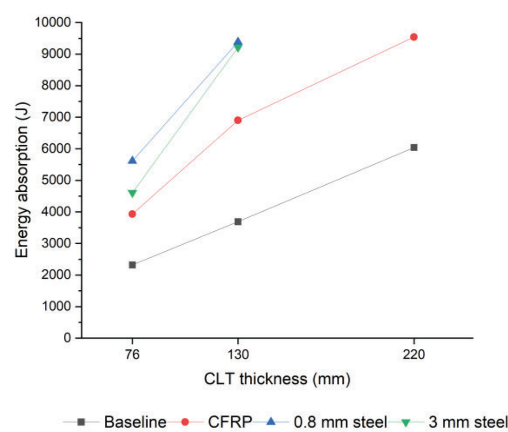

Figure 8. Variation of energy absorption by thickness of CLT

https://doi.org/10.52202/080513-0064

energy absorption capacity of the sample D10-CLT5-220-CFRP, might not reflect the maximum capacity up to the total collapse panel. Secondly, the premature rolling shear failure in CLT5-220-CFRP as opposed to tension failure in the baseline counterpart could have attributed to the reduction in increase.

4 – CONCLUSIONS

An experimental investigation on the impact behaviour of eleven CLT panels has been conducted and the consequences of hybridizing CLT panels with CFRP and steel under dynamic impact loading has been discussed in detail. The observations and analyses have resulted in the following key findings:

1. Collapse of unreinforced CLT panels demonstrates the lack of ductility and impact resistance and the need for hybridization to improve performance under dynamic loading.
2. Hybridizing CLT with steel sheets proved to significantly improve impact resistance and ductility by delaying onset of failure and energy dissipation while surface-mounted CFRP fabric had limited enhancement.
3. Natural defects and joints in CLT mainly influence the failure modes and stress concentrations on such areas should be considered when strengthening especially on surface-mounted CFRP fabrics in addition to the prevention of delamination.
4. Hybridization shifted failure modes from brittle tension failure toward more ductile and energy-dissipating failure modes, such as rolling shear and local yielding.
5. While increasing the thickness of CLT panels improved energy absorption, increasing the steel reinforcement thickness requires careful consideration. Increasing the thickness of steel reinforcement would not necessarily increase the impact resistance as the onset of rolling shear failure and separation remains a concern which prompts the need for further investigations and improvements against rolling shear and separation.

ACKNOWLEDGEMENTS

The authors gratefully acknowledge the support provided by technical officers Mr. Travis Marshall and Mr. Duncan Best, as well as undergraduate student Hayden Clay from the University of Wollongong, for their assistance in specimen fabrication and testing. This research was supported and funded by the Australian Research Council (ARC) under the Discovery Project DP210102499.

REFERENCES

[1] Australian Building Codes Board 2019, *National Construction Code 2019*, viewed 18/04/2023, https://ncc.abcb.gov.au/.

[2] Frühwald, E., et al., *Design of Safe Timber Structures - How Can we Learn from Structural Failures in Concrete, Steel and Timber?* 2007.

[3] Hansson, M. and H.J. Larsen, *Recent failures in glulam structures and their causes.* Engineering Failure Analysis, 2005. **12**(5): p. 808-818.

[4] Flores, N.R., R. Gentry, and L.K. Stewart, *Behavior and Damage Characterization of Impulsively Loaded Cross-Laminated Timber Panels.* Applied Sciences, 2022. **12**(23).

[5] Navaratnam, S., et al., *Bending and shear performance of Australian Radiata pine cross-laminated timber.* Construction and Building Materials, 2020. **232**: p. 117215.

[6] Poulin, M., et al., *Experimental and Analytical Investigation of Cross-Laminated Timber Panels Subjected to Out-of-Plane Blast Loads.* Journal of Structural Engineering, 2018. **144**(2).

[7] Lacroix, D.N. and G. Doudak, *Experimental and Analytical Investigation of FRP Retrofitted Glued-Laminated Beams Subjected to Simulated Blast Loading.* Journal of Structural Engineering, 2018. **144**(7): p. 04018089.

[8] Oliveira, D., C. Viau, and G. Doudak, *Behaviour of mass timber members subjected to consecutive blast loads.* International Journal of Impact Engineering, 2023. **173**.

[9] Karagöz İşleyen, Ü., et al., *Investigation of impact behavior of glulam beam strengthened with CFRP.* Structures, 2023. **51**: p. 196-214.

[10] Lopez-Molina, A. and G. Doudak, *Retrofit techniques for Cross-Laminated Timber (CLT) elements subjected to blast loads.* Engineering Structures, 2019. **197**.

[11] Goodarzi, A., S. Malek, and T. Tannert, *Experimental Investigation of the Shear Resistance of CLT Panels with Unreinforced and Reinforced End Notches.* Journal of Materials in Civil Engineering, 2025. **37**(1).

[12] Weaver, M.K., et al., *Blast Testing of Loaded Cross-Laminated Timber Structures*, in *Structures Congress 2018*. 2018. p. 400-411.

https://doi.org/10.52202/080513-0064

[13] Doudak, G., C. Viau, and D.N. Lacroix, *Proposed Design Methods for Timber Members Subjected to Blast Loads.* Journal of Performance of Constructed Facilities, 2022. **36**(3).

[14] Viau, C. and G. Doudak, *Behaviour and modelling of cross-laminated timber panels with boundary connections subjected to blast loads.* Engineering Structures, 2019. **197**.

[15] Viau, C. and G. Doudak, *Dynamic analysis methods for modelling timber assemblies subjected to blast loading.* Engineering Structures, 2021. **233**.

[16] Van Le, T., et al., *Dynamic increase factors for Radiata pine CLT panels subjected to simulated out-of-plane blast loading.* Engineering Structures, 2020. **225**.

[17] Sanborn, K., et al. *Towards a single degree of freedom (SDOF) model for predicting blast performance of cross-laminated timber*. in *Structures Under Shock and Impact XV*. 2018. WIT Press.

[18] Saatci, S. and F.J. Vecchio, *Effects of Shear Mechanisms on Impact Behavior of Reinforced Concrete Beams.* ACI Structural Journal, 2009. **106**(1): p. 78-86.

[19] Goldston, M., A. Remennikov, and M.N. Sheikh, *Experimental investigation of the behaviour of concrete beams reinforced with GFRP bars under static and impact loading.* Engineering Structures, 2016. **113**: p. 220-232.

[20] Saleh, Z., et al., *Damage assessment of GFRP bar reinforced ultra-high-strength concrete beams under overloading impact conditions.* Engineering Structures, 2020. **213**.

[21] Zhao, H., et al., *Performance of round-ended CFST columns under combined actions of eccentric compression and impact loads.* Engineering Structures, 2024. **301**.

[22] Zhao, H., et al., *Performance of circular CFDST members with external stainless steel tube under transverse impact loading.* Thin-Walled Structures, 2019. **145**.

[23] Goldston, M.W., et al., *Experimental investigations on the behavior of GFRP bar reinforced HSC and UHSC beams under static and impact loading.* Structures, 2019. **22**: p. 109-123.

[24] Banthia, N., et al., *Impact testing of concrete using a drop-weight impact machine.* Experimental Mechanics, 1989. **29**(1): p. 63-69.

[25] Fujikake, K., B. Li, and S. Soeun, *Impact Response of Reinforced Concrete Beam and Its Analytical Evaluation.* Journal of Structural Engineering, 2009. **135**(8): p. 938-950.

[26] Luo, C., et al., *Castellated steel beams under impact load.* Journal of Constructional Steel Research, 2022. **196**.

[27] Wang, F., et al., *Effect of impact loading on the dynamic response of steel beams with hexagonal web opening.* Thin-Walled Structures, 2022. **180**.

[28] Chen, Y., et al., *Experimental and numerical assessment of welded steel beam-column connections under impact loading.* Journal of Constructional Steel Research, 2020. **175**.

[29] Cao, A.S. and A. Frangi, *Dynamic strength increase of glued laminated timber beams subjected to impact loading*, in *10th International Network on Timber Engineering Research (INTER 2023)*, R. Görlacher, Editor. 2023, Timber Scientific Publishing, KIT Holzbau und Baukonstruktionen: Biel/Bienne, Switzerland. p. 309 - 330.